Send Orders for Reprints to reprints@benthamscience.net

The Open Mechanical Engineering Journal, 2014, *8*, 297-302

Open Access

Optimization Design on Triangle Plate of Auxiliary Frame of Mixer Truck

Sun Li*, Liu Yongchen and Fu Naiji

School of Traffic Engineering, Huaiyin Institute of Technology, Huai'an, 223003, China

Abstract: In order to solve the question of crack of the auxiliary frame of mixer truck, especially with the life of the triangle welding position is low, the triangle support of auxiliary frame optimization design is put forward Firstly, three dimensional structure model of auxiliary frame is established by Pro/E and the model is imported into HyperMesh software for meshing. The solver RADIOSS is used to calculate the maximum stress and the positions at the different full load conditions. Including the static, left front wheel lifted up by 210 mm, the right rear wheels (double) lifted up by 210 mm and the left front and right rear wheels lifted simultaneously up by 210 mm. Then the experimental vehicle test is performed. The test results and simulation results are compared and show a good consistency and the accuracy of the finite element model is validated. Then the three optimization design schemes of the triangle are put forward and the maximum stress of the optimal auxiliary frame are calculated in contrast with the original stress. The scheme 2 is found to be the most optimal, which provides an effective method for solving the fatigue of the auxiliary frame.

Keywords: Mixer Truck, optimization design, test, triangle plate of auxiliary frame.

1. INTRODUCTION

Due to cyclic stresses and strain endured from a variety of loading and unloading and complex roads systems, the cracks often emerge at the auxiliary frame of mixer trucks, especially at the welding joints on the triangle plate of the auxiliary frame, leading to a lot of repetitive repairs.. The auxiliary frame triangle plate structure optimization design is proposed. At present, there are many research papers studying the frame optimization design There are some research papers which propose to optimize the dump truck frame, front auxiliary frame and truck frame based on sensitivity analysis method. Some researches optimize the frame of light truck by multi-objective robust optimization method while others researchers analyze and optimize the auxiliary frames of motorcycle and fuel cell vehicles [1-10].

In order to solve the auxiliary frame crack problem of mixer truck, the 3D model is built by Pro/E software then it is imported into HyperMesh software for meshing, and the solution is solved by the RADIOSS analysis solver. Under different conditions and full load, the maximum stress of auxiliary frame triangle plate of the mixer truck is calculated. Then the experimental vehicle test is performed to verify the accuracy of the finite element model. The optimization design schemes of triangle plate are proposed, the maximum stress at possible emerging locations are calculated by finite element method FEM. Observing that the maximum stresses are decreased and the optimization goal is realized.

2. FEM ESTABLISHMENT AND STRENGTH CALCULATION

The auxiliary frame consists of two main girders and four beams. The beams and girders are welded to connect the front and rear supports. Reinforcements are welded to connect the longitudinal beams of auxiliary frame and the auxiliary frame is connected with the main frame by a U-shaped bolt.

First of all, the 3D model of auxiliary frame is designed by Pro/E software then the model is imported into the HyperMesh for meshing. The following points should be given extra attention: the vertex of any one plate and shell unit is the vertex of its adjacent unit; the unit shape are as regular as possible to avoid an edge which can be too long or too short and the inner angle can be too big or too small. Some positions are allowed to degrade to a triangular unit. The components of auxiliary frame are connected by welding. The welding position is simulated using rigid units, the finite element model of auxiliary frame consists of 201548 units and 199365 nodes, which are shown in Fig. (**1**).

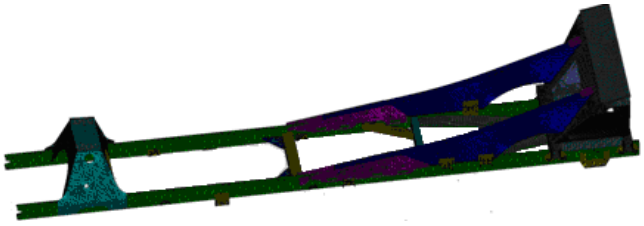

Fig. (1). FEM of auxiliary frame.

For the stress simulating of mixer truck under the different working condition, the boundary constraints of front axle points is at spring nodes of front axle and the boundary constraints of rear axle is at spring nodes of rear axle. When the full load working condition is simulated, the translational degree of freedom of the spring nodes in x, y

1874-155X/14

and z directions of front axle and rear axle are constrained. When the torsion working condition is simulated, the wheel height is lifted by 210 mm. The directional degree of freedom of the left front side and the right rear side spring node in z direction are are raised up by 210 mm, and the translational degrees of freedom of the left front side and right rear side spring nodes in z direction are raised up by 210 mm.

By RADIOSS calculation, the auxiliary frame strength of mixer truck of every working condition under full load status is shown in Fig. (**2**).

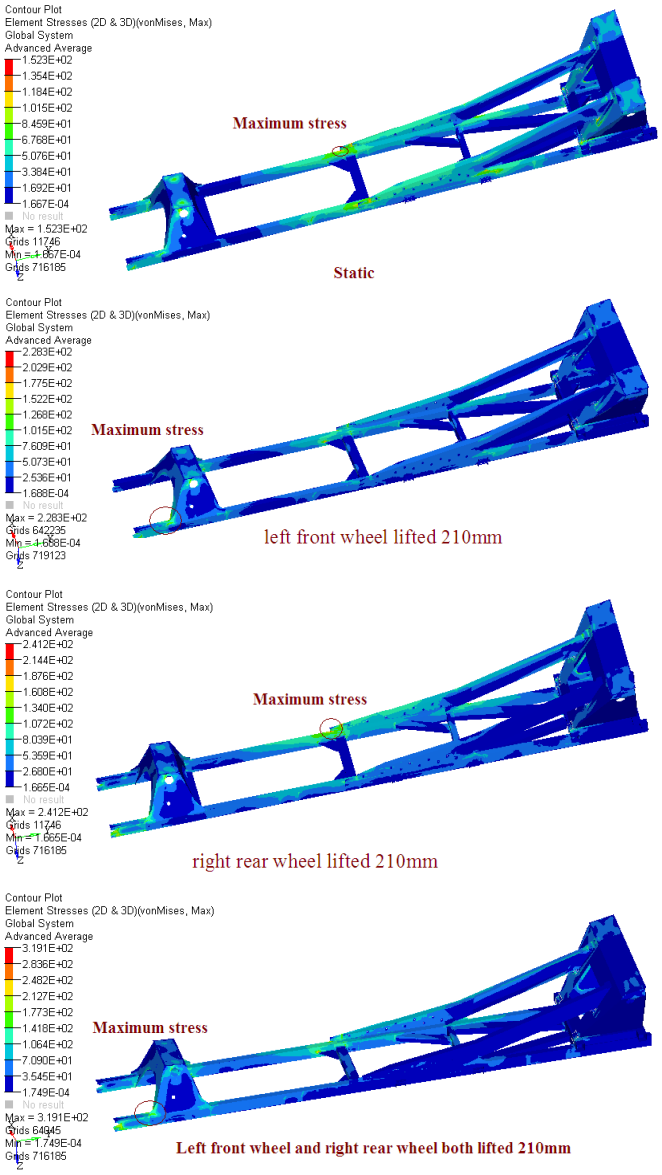

Fig. (2). Shows a auxiliary frame stress nephogram under full load condition.

Fig. (**2**) shows that under full load state, static state maximum stress of mixer truck auxiliary frame is 173.2 MPa, which occurs at the front connection welding position of the reinforcing rib and auxiliary frame. When the left front wheel is lifted up by 210 mm, the maximum stress of auxiliary frame is 340.0 MPa, which is located at the welding location of the left low side of front support with the inside the longitudinal beam of the auxiliary frame. When the right rear wheels are lifted up by 210 mm, the maximum stress is 281.2 MPa, which is at the front welding connection of the right reinforcement with the auxiliary frame. When left front wheel and right rear wheels are lifted up by 210 mm simultaneously, the maximum stress is 471.1 MPa, which is located at the welding location of the left low side of front support of the inside of auxiliary frame longitudinal beam.

3. STRESS TEST

In order to test the stress conveniently, the concentrated stress points by finite element simulation are selected to test, the marked diagram is shown as Fig. (**3**).

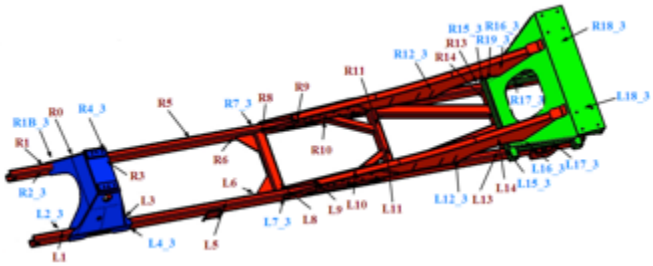

Fig. (3). Auxiliary frame key points.

X axis is the lateral of the frame to the right, Y axis is the reverse of the driving direction, Z axis is the vertical direction to the down, and the origin (0, 0, 0) is the midpoint of the front bottom surface center of the deputy main girder. There are 36 test points, including 21 shared unidirectional strain gauges, 15 three-direction strain gauges, and the total channels are 66, the test instrument that are used has 63 channels, as shown in Fig. (**4**). So there are 3 more channel conversion modules needed to reach the total quantity.

One-way test points in the test are labelled L and R (left is L, right is R), three-way test points are labelled L-3 and R-3 and the symmetric points named L1-R1, L2_3-R2_3. L4_3 is malfunctioning in the test, so the test data is not desirable. Due to the limit of channel number, the R1B_3 and R19_3 is not tested, the test points patches are shown in Fig. (**4**).

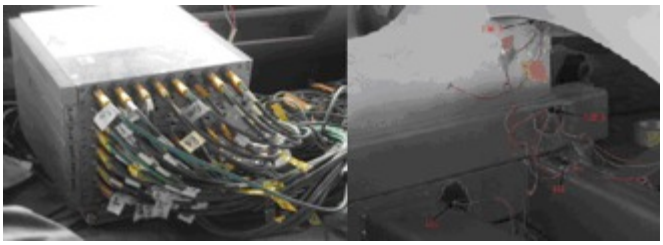

Fig. (4). Test equipment and actual location of test points.

There are some things that should be noted in the test, the test equipment is debugged to zero, then 12 m^3 of sand and water are placed into the mixing bowl and used as full load to test the experimental data.. When torsion experiment is carried out, as shown in Fig. (**5**), right rear wheels of mixer truck are first driven on convex platform to test the data as if the right rear wheels are lifted up by 210 mm. Then left front wheels are driven on the convex platform, data is measured when left front wheels are lifted up by 210 mm. Finally, left front and right rear wheels are derived on convex platform and data is measured when both wheels are lifted up by 210 mm.

Fig. (5). Torsion test.

Experimental results are compared with the FEM simulation results and the relative error formula is:

Relative error = (simulation result-test result) / test result x100%.

Data comparison results are shown in Tables **1-4**. In the tables, ER is the experiment results, SR is the simulation results, RE is the relative error, F is the fault.

By above Comparison, it can be found that the relative error is small in the strain under bending and torsion test. Only R7_3 simulated value is more larger under full load bending and L7_3 simulated value are small under the diagonal lift, which is mainly due to asymmetrical stress caused by the frame integral center-of-gravity shift, combined with the actual left and right asymmetrical patch position which leads to the error between the simulation and experimental values. The error of strain gauges is mainly caused by the different stress modes under different working conditions of the actual frame. At the same time, the concrete quality distribution within the mixing drum is non-uniform, leading to the center-of-gravity offset, making the frame stress asymmetrical, so that the symmetry degree of

Table 1. Full load bending results and comparison with FEM simulation results.

No.	L1	L2_3	L3	L4	L5	L6	L7_3	L9	L10	L11	L12_3	L13	L14	L15_3	L16_3	L17_3	L18_3	R0
ER	-82.73	153.5	27.58	F	38.09	9.35	68.07	87.66	-5.02	-0.81	64.62	6.60	17.98	35.23	77.85	67.45	33.06	-34.83
SR	-38.71	149.6	17.78		45.38	9.35	68.17	91.45	-4.55	-0.45	51.4	7.716	17.25	37.3	84.78	63.31		-30.86
RE (%)	-53.21	-2.55	-35.53		19.13	-0.02	0.15	4.33	-9.30	-44.64	-20.46	16.96	-4.05	5.87	8.90	-6.14		-11.41
No.	R1	R2_3	R3	R4_3	R5	R6	R7_3	R9	R10	R11	R12_3	R13	R14	R15_3	R16_3	R17_3	R18_3	
ER	-72.52	120.4	-6.21	42.20	49.86	23.48	23.74	96.68	-33.5	2.73	98.13	-19.1	3.84	24.64	72.89	78.64	28.42	
SR	-36.52	129.4	-7.77	31.68	50.56	22.88	48.9	96.43	-4.17	11.05	106.1	-4.38	3.99	25.44	65.38	68.7		
RE (%)	-49.64	7.48	25.24	-24.94	1.41	-2.56	106.0	-0.26	-87.6	305.4	8.12	-77.1	3.97	3.23	-10.31	-12.64		

Table 2. Experiment results comparison with simulation result when left front wheels lifted up under full load.

No.	L1	L2_3	L3	L4	L5	L6	L7_3	L9	L10	L11	L12_3	L13	L14	L15_3	L16_3	L17_3	L18_3	R0
ER	-123.2	255.00	56.58	failure	37.79	9.43	50.40	74.27	-12.73	-5.28	60.21	4.94	17.01	31.80	63.69	44.29		-14.54
SR	-60.64	253.40	59.81		35.70	59.81	53.49	66.77	-0.37	-5.23	50.46	4.03	17.30	30.50	66.55	43.79		-14.94
RE (%)	-50.76	-0.63	5.70		-5.53	534.46	-5.78	-10.10	-97.06	-1.07	-16.19	-18.40	1.70	-4.08	4.49	-1.14		2.76
No.	R1	R2_3	R3	R4_3	R5	R6	R7_3	R9	R10	R11	R12_3	R13	R14	R15_3	R16_3	R17_3	R18_3	
ER	-52.49	50.39	-28.95	83.41	63.39	36.17	71.90	114.91	8.38	6.27	104.26	-17.52	2.81	26.19	81.60	110.07		
SR	-9.78	57.06	-30.44	79.65	50.38	41.63	73.14	102.60	-22.27	5.45	109.20	-3.89	2.10	26.86	81.22	105.72		
RE (%)	-81.36	13.23	5.15	-4.51	-20.52	15.04	1.72	-10.71	-137.6	-13.12	4.73	-77.82	-25.32	2.57	-0.46	-3.95		

Table 3. Experiment results Comparison with simulation result when right rear wheels lifted up under full load.

No.	L1	L2_3	L3	L4	L5	L6	L7_3	L9	L10	L11	L12_3	L13	L14	L15_3	L16_3	L17_3	L18_3	R0
ER	-120.7	256.08	5.95	F	31.14	40.49	52.03	92.90	-5.89	9.93	91.86	-4.518	24.34	56.32	89.80	27.36	34.46	-14.25
SR	-50.37	210.90	28.82		59.11	48.97	56.32	103.50	-5.09	7.99	87.52	-5.64	16.14	55.49	87.37	28.86		-16.73
RE (%)	-58.26	-17.64	384.34		89.84	20.93	8.24	11.41	-13.68	-19.47	-4.73	25.16	-33.70	-1.47	-2.70	5.47		17.38
No.	R1	R2_3	R3	R4_3	R5	R6	R7_3	R9	R10	R11	R12_3	R13	R14	R15_3	R16_3	R17_3	R18_3	
ER	-42.17	41.73	13.91	71.01	63.89	-13.34	67.16	88.34	-24.74	-5.05	59.11	1.87	-1.43	24.83	70.52	102.00	25.18	
SR	-45.92	37.83	15.61	65.07	77.61	24.48	79.54	99.60	-5.74	-6.90	58.73	4.79	-1.63	25.84	77.84	115.39		
RE (%)	8.90	-9.34	12.21	-8.37	21.47	-283.46	18.44	12.75	-76.79	36.46	-0.64	155.82	14.17	4.08	10.38	-11.60		

Table 4. Experiment results comparison with simulation result when diagonal wheels lifted up under full load.

No.	L1	L2_3	L3	L4	L5	L6	L7_3	L9	L10	L11	L12_3	L13	L14	L15_3	L16_3	L17_3	L18_3	R0
ER	-173.2	437.11	64.69	F	39.37	23.50	72.12	77.37	-16.20	2.87	85.22	-4.20	24.30	55.07	79.67	19.82	33.51	1.04
SR	-71.93	487.30	61.08		46.39	38.34	43.87	76.41	-2.93	10.81	83.95	-3.87	9.28	55.45	87.38	22.57		2.18
RE (%)	-58.48	11.48	-5.59		17.82	63.14	-39.17	-1.24	-81.89	276.74	-1.49	-7.89	-61.81	0.69	9.67	13.88		109.14
No.	R1	R2_3	R3	R4_3	R5	R6	R7_3	R9	R10	R11	R12_3	R13	R14	R15_3	R16_3	R17_3	R18_3	
ER	-22.80	39.43	-41.36	118.66	65.80	7.95	101.31	106.42	-17.63	0.81	70.14	-0.62	-4.50	27.64	81.25	148.24	28.51	
SR	-0.81	84.51	-46.47	106.90	73.41	9.69	106.80	118.00	14.95	1.26	71.67	-0.41	-3.18	27.64	74.17	148.40		
RE (%)	-96.43	114.35	12.37	-9.91	11.57	21.90	5.42	10.89	-184.8	55.86	2.17	-34.33	-29.45	0.00	-8.71	0.11		

test results is poor. In addition to the phenomenon where part of strain gauges emerge slightly askew when the strain gauges are slicked, some test points simulation results have more error than test results. Above all, most of the simulation results have relatively little error than experimental results, so the finite element model and simulation results are reasonable.

4. TRIANGLE PLATE OPTIMIZATION DESIGN

Due to larger stress amplitude of the A5 and A6 position, can reach 231.03 MPa and 190.15 MPa, which will lead the life of welding joint of A5 and A6 fields being small, as shown in Fig. (**6**).

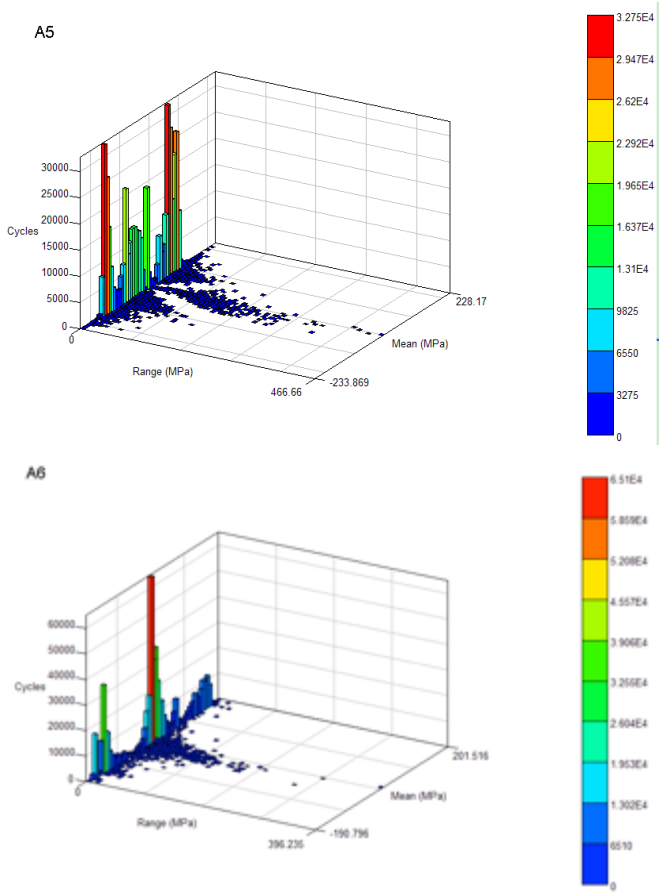

Fig. (6). The mean amplitude of A5 and A6 points.

In order to reduce the stress amplitude of A5 and A6 field, the triangle plate structure optimization is proposed, the specific scheme is as following:

1) Scheme 1: the triangle extends 50 mm to the vehicle lateral direction;

2) Scheme 2: the triangle extends 50 mm to the vehicle driving direction;

3) Scheme 3: the triangle extends 50 mm respectively to the driving direction and vehicle lateral direction.

The schematic diagram is shown in Fig. (**7**).

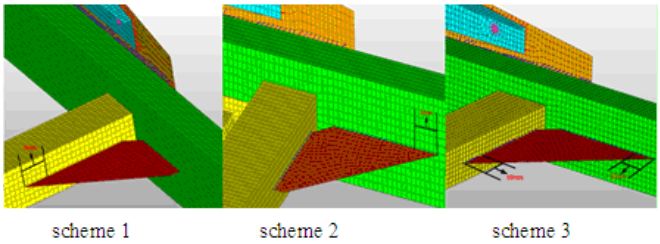

Fig. (7). Optimization scheme.

5. STRESS ANALYSIS OF THE OPTIMIZED TRIANGLE PLATE

A5 and A6 field Stress analysis of three optimization design schemes and the original triangle plate are done, the stress contours are shown in Figs. (**8**, **9**).

From Fig. (**8**), under full load conditions, the static maximum stress of mixer truck auxiliary frame is 152.3 MPa, which is concentrated at the front welding connection of the reinforcement with auxiliary frame. When left front wheel is lifted up by 210 mm, the maximum stress of auxiliary frame is 228.3 MPa, which is concentrated at the welding location on the left low side of the front support with the longitudinal beam inside of the auxiliary frame. When right rear wheels are lifted up by 210 mm, the maximum stress of auxiliary frame is 241.2 MPa, which concentrated at the front welding connection of the right reinforcement of the auxiliary frame. When left front wheel and right rear wheels are lifted up at the same time by 210 mm, the maximum stress of auxiliary frame is 319.1 MPa, which concentrated at the welding location of left low side of the front side with longitudinal beam inside the auxiliary frame.

From Fig. (**8**), the stress of A5 point under bending condition in scheme 1 is exhibited reduced reduction, but the

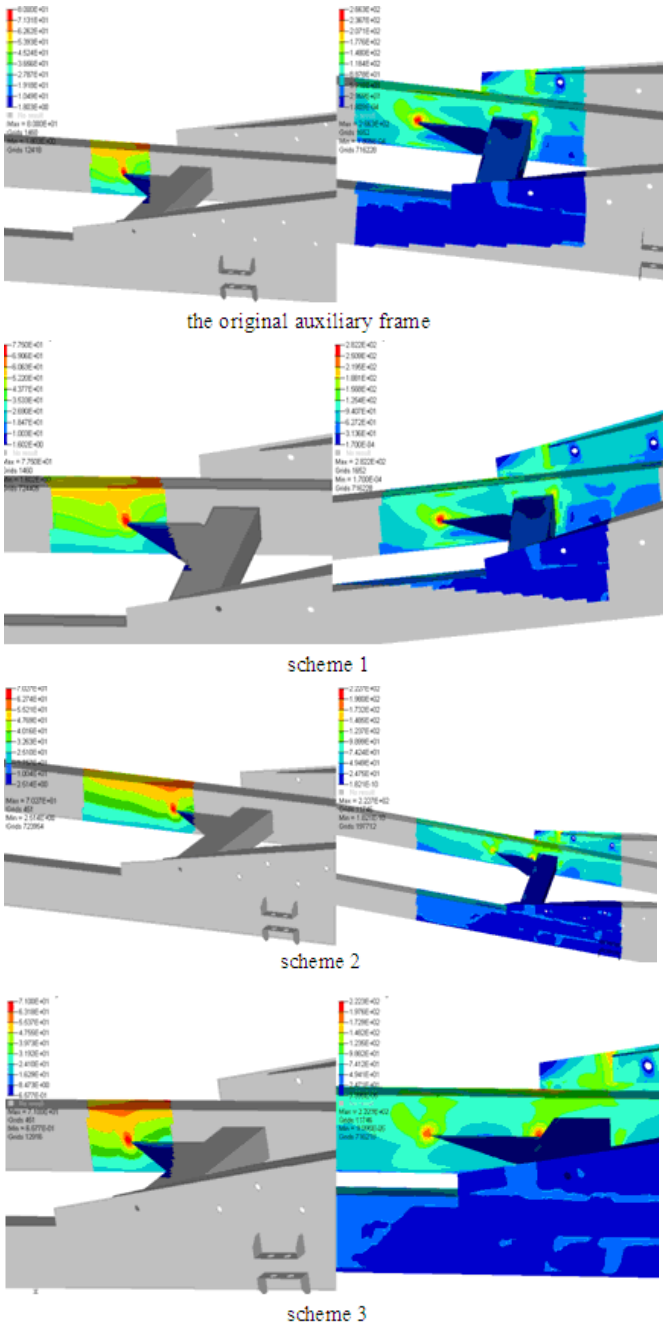

Fig. (8). A5 field stress nephogram.

stress of A5 point under torsion condition shows a large increase. The stress amplitude can increase, which is undesirable. The stress of A5 point under bending condition in scheme 2 and scheme 3 is decreased and the stress decreases under torsion condition, the stress amplitude is smaller than the original, from 186 MPa to 152 MPa. So the two schemes are desirable, but considering the complexity of the process and the production cost, scheme 2 is selected ultimately.

From Fig. (**9**), the stress amplitude of scheme 1 is 80 MPa, the stress amplitude of scheme 2 is 92 MPa, the stress amplitude of scheme 3 is 95 MPa, the original stress amplitude is 98 MPa, all are lower and desirable.

Considering comprehensively the influences of A5 and A6, the final option is scheme 2.

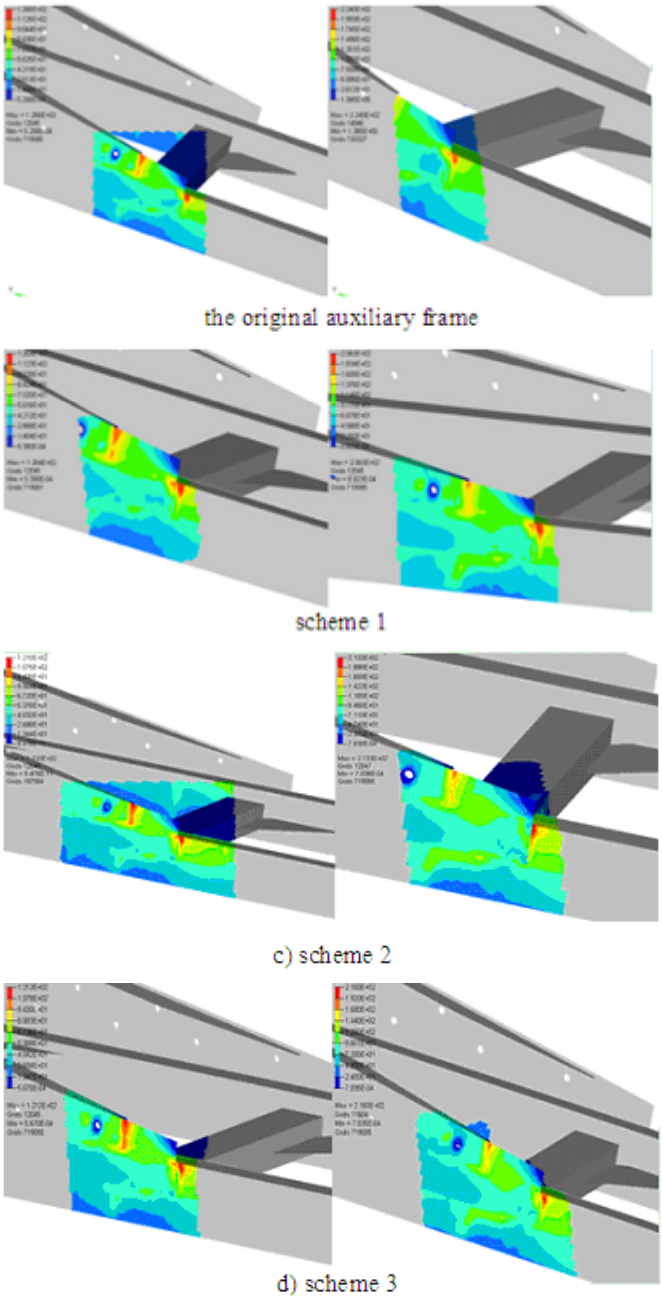

Fig. (9). A6 field stress nephogram.

CONCLUSION

In order to solve the crack problem which often emerges in the auxiliary frame of a mixer truck, especially, concerning the reduced durability of the welding joint of the triangle plate. The 3D model is designed in Pro/E, imported into HyperMesh to mesh, then the stress is calculated by RADIOSS analysis solver and the real vehicle stress test is conducted. This research compared the experimental stress test results of the auxiliary frame under different conditions with the simulation results to verify the finite element model and the accuracy of the simulation results. The three optimization design schemes of the triangle plate are proposed. The same FEM is used to simulate and compare the optimization effects of different schemes, the following conclusions are obtained:

1) With real vehicle stress testing, the relative error of most simulation results are compared with the experimental results, so the finite element model and the simulations are valid.

2) In three triangle plate optimization schemes, the stresses of A5 and A6 points are under the bending and torsion conditions, the optimization scheme 2 is selected.

CONFLICT OF INTEREST

The authors confirm that this article content has no conflict of interest.

ACKNOWLEDGEMENTS

The authors gratefully acknowledge the sponsored by Qing Lan Project, the supports from Natural Science Foundation of Jiangsu Province (BK2011405), and the Natural Science Foundation of the Jiangsu Higher Education Institutions of China (13KJB580001).

REFERENCES

[1] K.W. Jeon, K.B. Shin, and J.S. Kim, "A Study on fatigue life and strength of a GFRP composite bogie frame for Urban Subway Trains", *in 11th International Conference on the Mechanical Behavior of Materials*, 2011, vol. 10, 2405-2410.

[2] S.S. Rane, A. Srividya, and A.K. Verma, "Multi-objective reliability based design optimization and risk analysis of motorcycle frame with strength based failure limit", *International Journal of System Assurance and Engineering Management*, vol. 3, pp. 33-7, 2012.

[3] Q. Feng, "Research on Lightweight Design of Vice-Frame Structure of Fire-engine on Basis of ANSYS", *Computer-aided Industrial Design & Conceptual Design*, vol. 2, pp.1347-4, 2010.

[4] H. T. Liu, and T. Y. Wang, "Experimental study and finite element analysis of the seismic behaviors for steel fiber reinforced high-strength concrete frame exterior joints" *Advanced Materials Research*, vol. 295-297, pp.1499-6, 2011.

[5] W. Tie, Z. Zhen, and C. Zhi, "Optimization design of truck frame based on the sensitivity analysis", *Journal of TaiYuan University of Technology*, vol. 43, pp. 610-6, 2012.

[6] M. Xiaokang, L. Qiang, and Z. Zhijian, "Structure analysis and optimization design for aluminum alloy frame of energy-saving vehicle", *Machinery Design & Manufacture,* vol. 4, pp. 16-3, April 2012.

[7] Z. Caichao, Z. Jin, and Z. Weimin, "Structureal Optimization of Motorcycle Frame", *Automotive Engineering*, vol. 31, pp. 78-4, 2009.

[8] Y. Chengxiang, H. Zhigang and Q. Xiaobin, "Robust and multipurpose optimum design of light-truck", *Machinery Design & Manufacture,* vol. 8, pp. 56-3, 2007.

[9] W. Jian, Y. Zhuoping, and N. Guobao, "Strength and modality analysis on structure of fuel cell vehicle subframe", *Journal of Machine Design*, vol. 24, pp. 24-3, 2007.

[10] Y. Min, H. Junjie and W. Hao, "Sensitivity analysis and structural optimization of truck frame", *Journal of HeFei University of Technology*, vol. 34, pp. 993-4, 2011.

Received: July 25, 2014 Revised: August 4, 2014 Accepted: August 4, 2014